CHAPTER 5: MODEL SIMULATION AND VERIFICATION

5.1 INTRODUCTION

The aim of this chapter is to verify the combined model with data from an actual tap. Data that was obtained from measurements at Iscor Vanderbijlpark works can be used to do this in two ways. Firstly, model input trajectories of supply materials and energy sources can be matched exactly to that of the actual tap. Secondly, parameters within the state space model can be adjusted to give comparable results. The applicable data is given in Appendix B.

As elements such as phosphorus and manganese are omitted from the model, the carbon and silicon impurities are slightly increased to account for the mass balance of oxidising reagents that would have reacted with the omitted elements had they been included. The same applies to FeO and SiO_2 since products such as Fe_2O_3 or Al_2O_3 are not included in the model.

In Section 5.2 the EAF operation is discussed. In Section 5.3 the disturbance model is developed. In Section 5.4 a simulation without model adjustment is shown. In Section 5.5 the method for model adjustment is discussed. In Section 5.6 the adjusted model simulation is compared to the actual tap data as well as the unadjusted model simulation.

5.2 EAF OPERATION

Conditions for the actual tap under consideration are described in this section. At the end of the previous tap 20 ton hot heel was left in the furnace, with negligible impurities. The following materials were added from two large vessels: (T = 0 when the arc is switched on for the first time.)

- 53.5 ton scrap of high purity type, with less than 0.5% impurities, added at T = -1 min;
- 8 ton burnt lime and 3.5 ton doloma, added together with the scrap at T = -1 min;
- 65 ton hot metal (Liquid), with 4.4% carbon and 1.1% silicon, added at T = 10 min.

The following materials were added continuously throughout the process at constant feed rates by means of conveyer belts (total values are given):

- 35 ton DRI in total, with 82.5% metalization, 4.5% SiO_2 and 13% FeO;
- 2.5 ton burnt lime in total, 1.5 ton doloma in total and 0.5 ton anthracite in total.

The following feeds were injected continuously throughout the process at constant feed rates by means of injection lances (total values are given):

- 0.1 ton graphite in total, with air used as the carrier gas;
- 4220 Nm^3 oxygen in total.

The total energy input was 70605 kWh. The total iron content of the added inputs is 144 ton, 53.5 ton from the scrap, 61.5 ton from the hot metal and 29 ton from the DRI. The hot heel is not taken into account, because at the end of this tap the same mass of hot heel will be left in the furnace. To verify that this particular tap is typical, the specific energy and oxygen consumption are compared to the industry average. This particular tap used 490.3 kWh/ton electrical energy and 29.3 Nm^3/ton oxygen which is close to the industry average (500 kWh/ton, 30 Nm^3/ton) [30,40].

The following is a selected list of events that describe the tap. Rates have been converted from their units in the data sheets to units of kg/s or MW:

- T = -1 min: Scrap, lime and doloma added;
- T = 0 min: Arc switched on, 48.9 MW;
- T = 4 min: Arc switched off;
- T = 10 min: Hot metal added;
- T = 15 min: Oxygen injection started, 2.1 kg/s;
- T = 17 min: Arc switched on, 48.9 MW;
- T = 22 min: Slag conveyer belt started, 1.21 kg/s slag and 0.15 kg/s anthracite;
- T = 33 min: Graphite injection started, 0.42 kg/s;
- T = 35 min: DRI conveyer belt started, 11.2 kg/s;
- T = 37 min: Graphite injection stopped;
- T = 56 min: DRI feed rate increased to 33.6 kg/s;
- T = 59 min: Oxygen injection stopped;
- T = 61 min: DRI feed rate reduced to 11.2 kg/s;
- T = 73 min: DRI feed rate increased to 22.4 kg/s;
- T = 75 min: DRI conveyer belt stopped;
- T = 77 min: Slag conveyer belt stopped;
- T = 82 min: Arc switched off;
- T = 83 min: Steel tapped.

5.3 DISTURBANCE MODEL

The simulation starts when the furnace roof is closed for the last time. On the event-list given above, this is done at T = 15 minutes, when the oxygen injection is started. Before this the furnace roof is pivoted open to allow the hot metal charge. During the charge the valve to the water-cooled duct is closed, while the valve to the overhead canopy is opened in order to capture gas escaping from the open EAF. While the overhead canopy is in use, it is not possible to do any control on the off-gas at all. In addition, the model does not apply to times when the EAF roof is open. Consequently, the simulation is only started at T = 15 minutes, when the furnace roof is closed and

the oxygen injection is started. At this time the valve to the water-cooled duct is opened, and the overhead canopy is no longer used. The total simulation time is 65 minutes (until T = 80 above).

The anthracite is added to the slag to react with the FeO and make the slag foam [30] in order to limit the nitrogen pickup in the steel. In this regard it has exactly the same role as the graphite injection. The anthracite is not pure carbon however, but consists of approximately 80% carbon and 15% ash. It also contains small percentages of oxygen, hydrogen and water. To accommodate this input in the model (the model assumes pure graphite injection), the anthracite is multiplied by a coefficient of 0.8 and added to the graphite injection. The ash and other impurities are ignored.

The power efficiency of the electrical system is assumed to be 80% [29], i.e. 80% of the energy input from the transformer reaches the steel melt. Consequently, the arc power is multiplied by a factor of 0.8 in the disturbance model. The disturbance model consists of the profiles for the disturbance inputs that are the same as for the actual EAF tap. Note that the simulation time is 15 minutes less than the actual tap time. The profiles for those inputs that are treated as disturbances in this dissertation are as follow:

- Fig.5.1 shows the profile for the electrical power (multiplied by efficiency factor, $\eta = 0.8$);
- Fig.5.2 shows the oxygen injection profile;
- Fig.5.3 shows the DRI charge rate profile;
- Fig.5.4 shows the slag charge rate profile;
- Fig.5.5 shows the equivalent carbon feed rate profile.

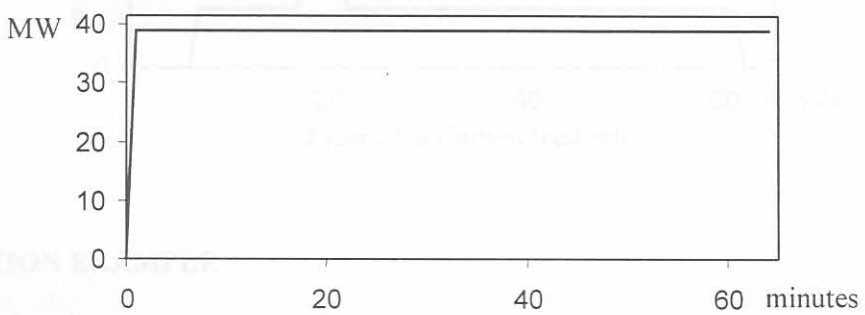

Figure 5.1 Arc electrical power input

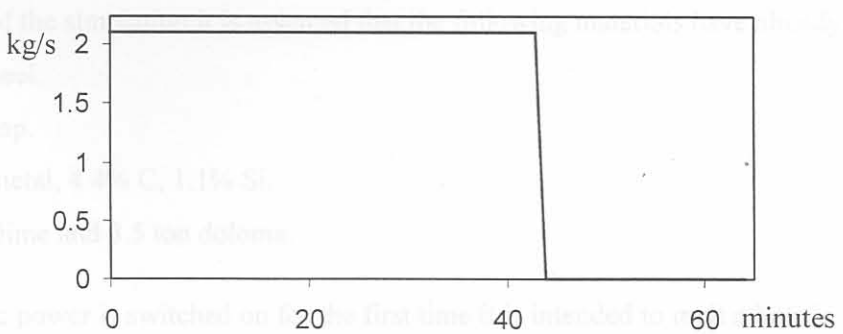

Figure 5.2 Oxygen injection

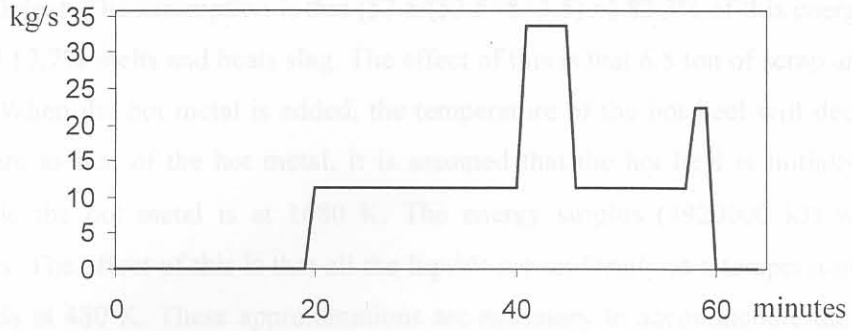

Figure 5.3 DRI charge rate

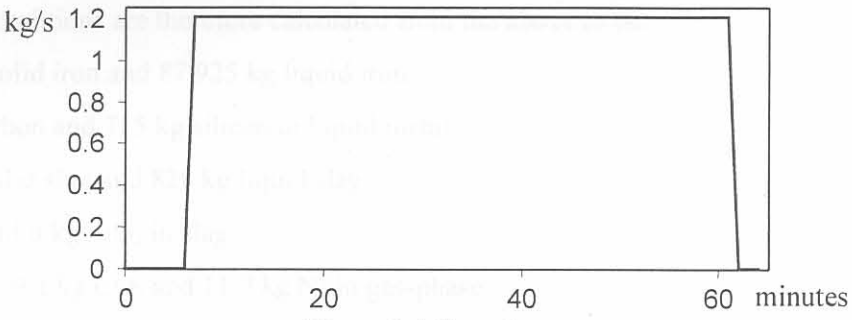

Figure 5.4 Slag charge rate

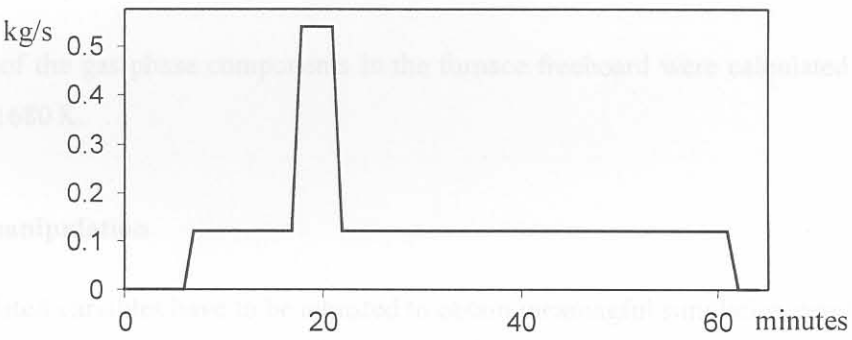

Figure 5.5 Carbon feed rate

5.4 SIMULATION EXAMPLE

5.4.1 Initial Conditions

At the start of the simulation it is assumed that the following materials have already been added:

- 20 ton hot heel.
- 53.5 ton scrap.
- 65 ton hot metal, 4.4% C, 1.1% Si.
- 8 ton burnt lime and 3.5 ton doloma.

When the arc power is switched on for the first time it is intended to melt a hole in the scrap. At this stage 9360000 kJ is delivered. The arc efficiency is already accounted for by using an

efficiency coefficient. The assumption is that (53.5/(53.5+8+3.5) =) 82.3% of this energy melts and heats scrap, and 17.7% melts and heats slag. The effect of this is that 6.5 ton of scrap and 820 kg of slag will melt. When the hot metal is added, the temperature of the hot heel will decrease to the same temperature as that of the hot metal. It is assumed that the hot heel is initially at 1980 K (~1707°C) while the hot metal is at 1680 K. The energy surplus (4920000 kJ) will heat the remaining solids. The effect of this is that all the liquids are uniformly at a temperature of 1680 K and all the solids at 480 K. These approximations are necessary to accommodate the actual EAF conditions within the framework of the model.

The initial conditions are therefore calculated from the above to be:

- 47 000 kg solid iron and 87 925 kg liquid iron
- 2860 kg carbon and 715 kg silicon in liquid metal
- 10680 kg solid slag and 820 kg liquid slag
- 0 kg FeO and 0 kg SiO_2 in slag
- 17.4 kg CO, 9.1 kg CO_2 and 11.7 kg N_2 in gas-phase
- Liquids at 1680 K and solids at 480 K
- Relative furnace pressure starting at 0 Pa.

The masses of the gas-phase components in the furnace freeboard were calculated assuming a temperature of 1680 K.

5.4.2 Off-gas manipulation

The manipulated variables have to be adjusted to obtain meaningful simulation results. The slip-gap size is kept constant at a value of 0.33 m. The fan power is kept at 0.8 MW until simulation time t = 50 minutes, when it is decreased to 0.4 MW.

5.4.3 Simulation results

Fig.5.6 shows the liquid metal mass and the scrap mass on the same graph. Note that the addition of DRI (t=41) directly increases the liquid metal mass. Before DRI addition it is evident that the rate of increase of liquid metal mass is equal to the rate of decrease of the scrap mass.

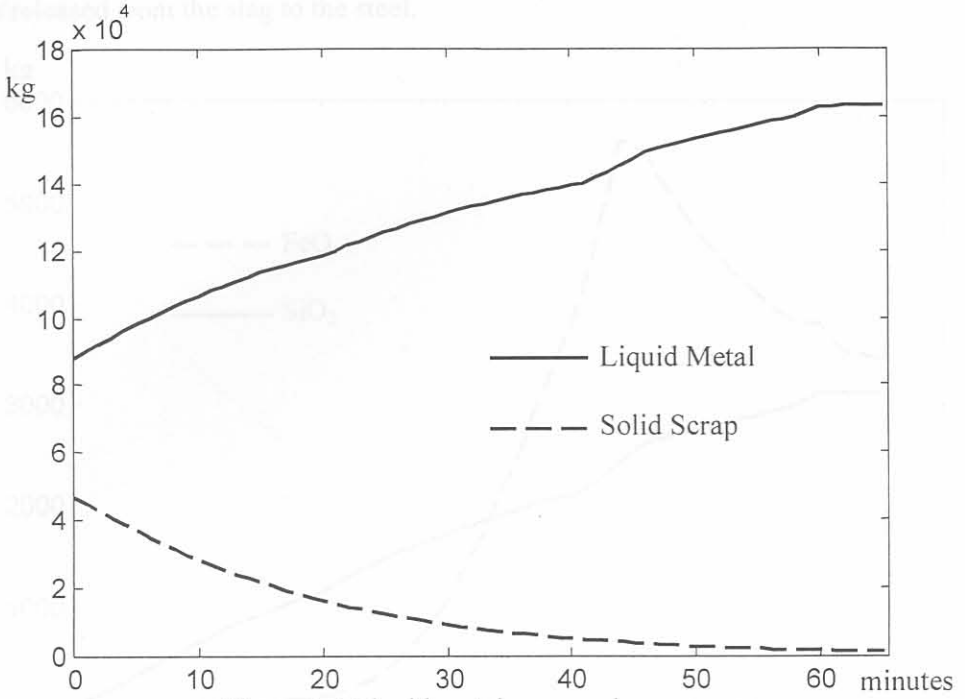

Figure 5.6 Liquid metal mass and scrap mass

Fig.5.7 shows the mass of carbon and silicon in solution in the liquid metal. Note that the silicon reaches the equilibrium concentration much quicker than the carbon. The explanation for this is simply that silicon is much more reactive in a basic slag environment.

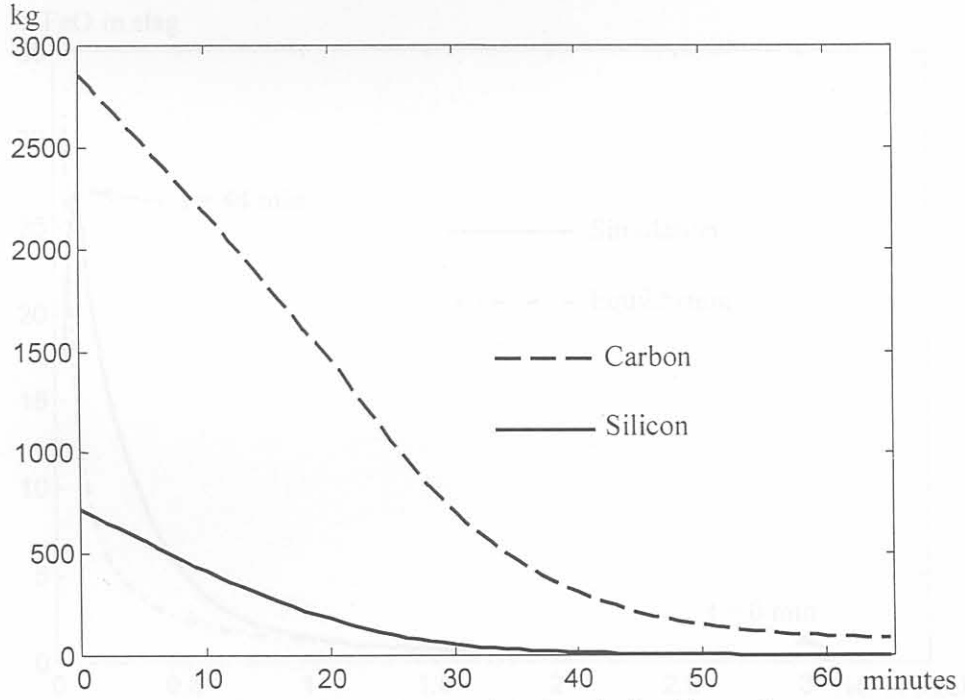

Figure 5.7 Silicon and Carbon in liquid metal

Fig.5.8 shows the SiO_2 and FeO in solution in the liquid slag. Note that the SiO_2 does not react with anything after it entered the slag-phase as the basic slag environment prevents silicon from re-entering the steel. However, the FeO reacts with carbon in the steel and in the graphite injection,

and iron is released from the slag to the steel.

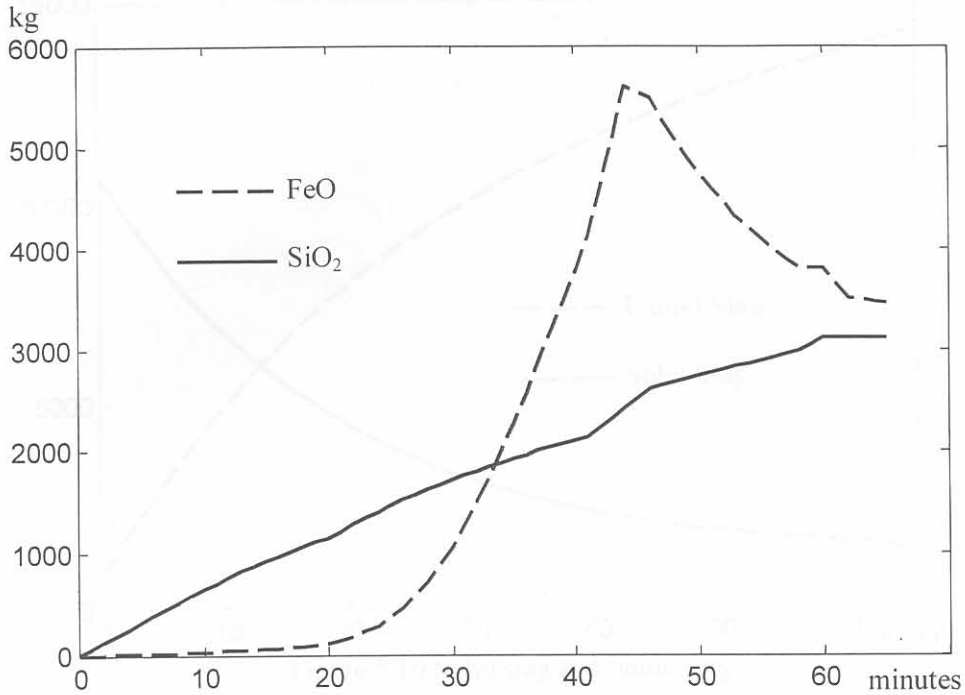

Figure 5.8 SiO_2 and FeO in slag

Fig.5.9 shows the relationship between the FeO mass percentage in the slag and the carbon mass percentage in the steel melt. The equilibrium relationship is shown on the same graph.

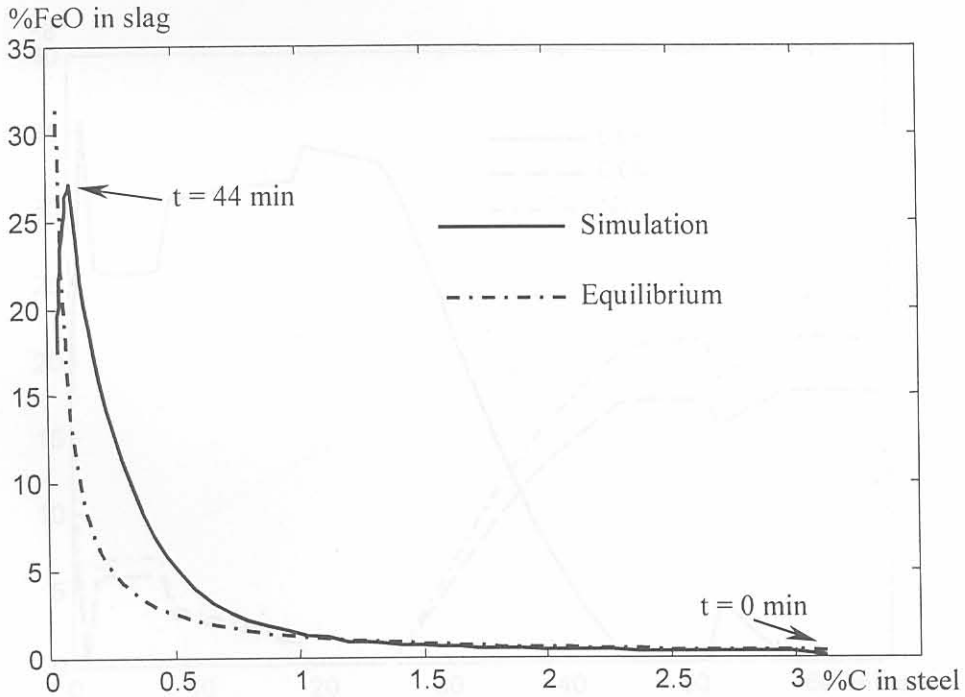

Figure 5.9 %FeO in slag against %C in steel

Fig.5.10 shows the masses of the solid and liquid slag. Note that in this dissertation the FeO and SiO_2 components are excluded from the liquid slag mass, although they are accounted for in thermo-chemical calculations. This means that the liquid slag mass denotes CaO and MgO only.

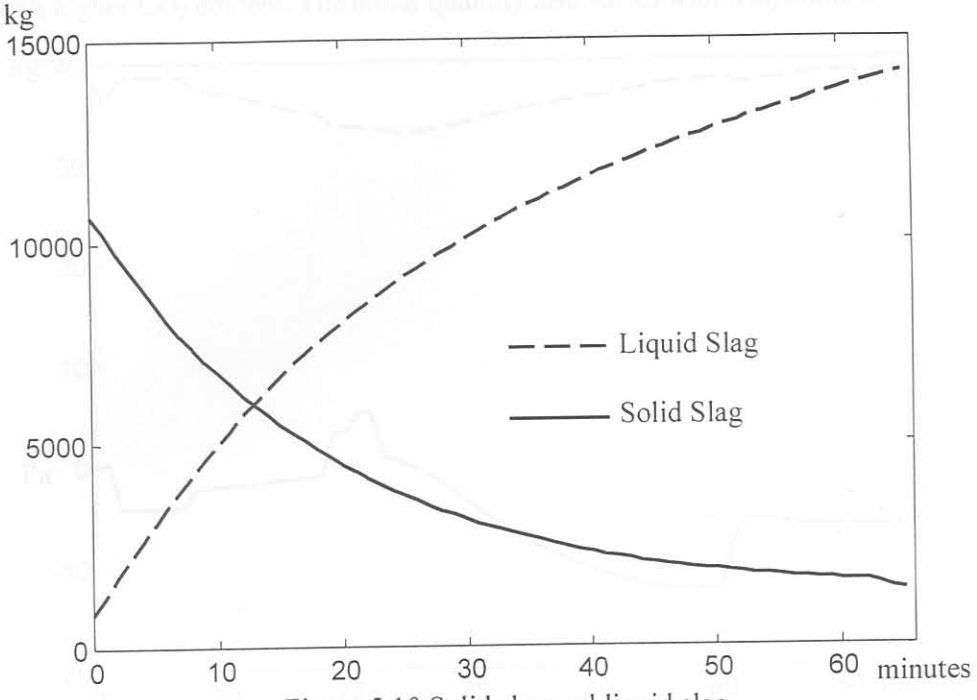

Figure 5.10 Solid slag and liquid slag

Fig.5.11 shows the three gas components together. In the first half of the simulation (t<30), the oxygen injection causes carbon monoxide production. When the oxygen injection stops, the conditions in the furnace are more favourable for carbon to combust directly to carbon dioxide.

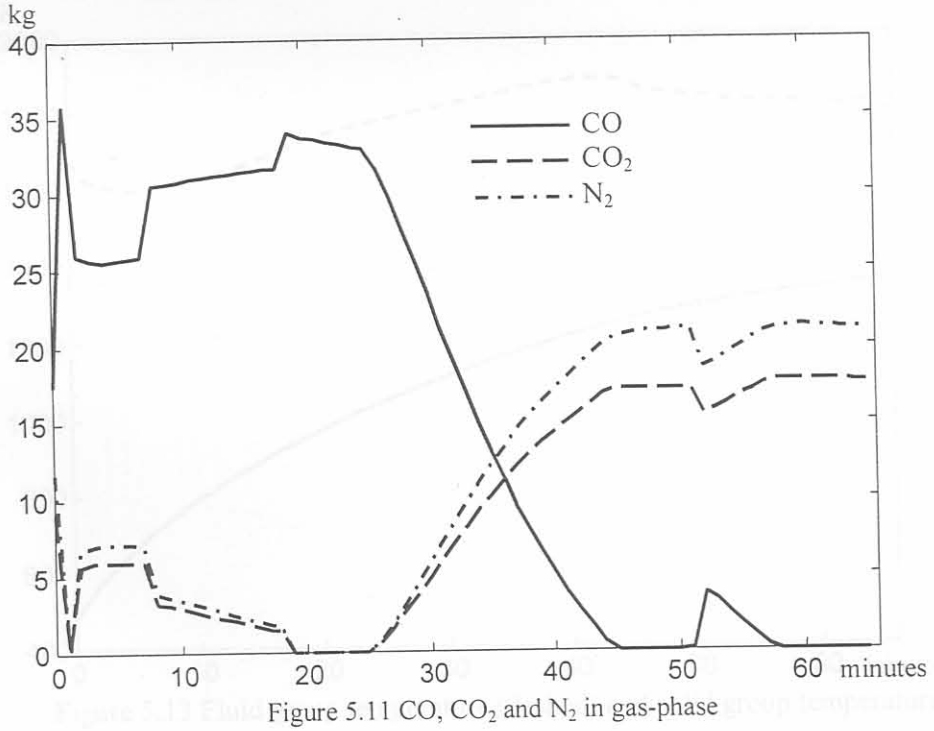

Figure 5.11 CO, CO_2 and N_2 in gas-phase

Fig.5.12 shows the sum of the gas-masses, together with the relative pressure of the furnace. Although the ideal gas law determines that the total molar quantity remains constant in the furnace, the mass will vary due to gas composition changes. CO_2 is a heavy gas and the total gas mass thus

increases with higher CO_2 content. The molar quantity also varies with temperature.

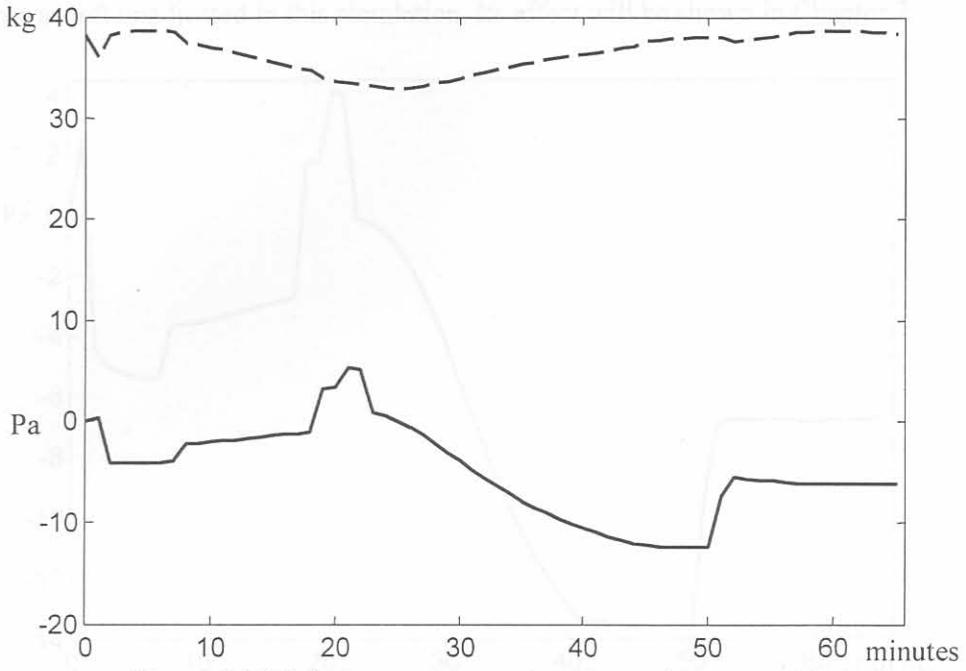

Figure 5.12 Relative pressure and total gas-phase mass (dashed)

Fig.5.13 shows the liquid metal temperature and the scrap temperature. Note that the scrap temperature approaches the liquid metal temperature gradually as the scrap is melted away.

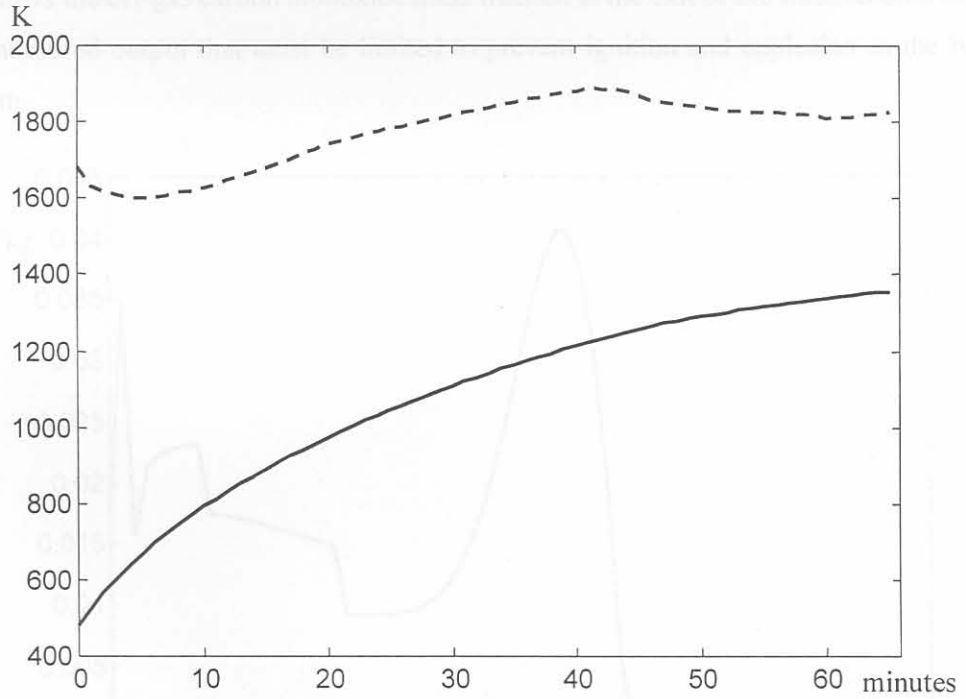

Figure 5.13 Fluid group temperature (dashed) and solid group temperature

Fig.5.14 gives a closer look at the relative pressure, which is also a measured output. Note that the slip-gap was left unadjusted in this simulation. Its effect will be shown in Chapter 7.

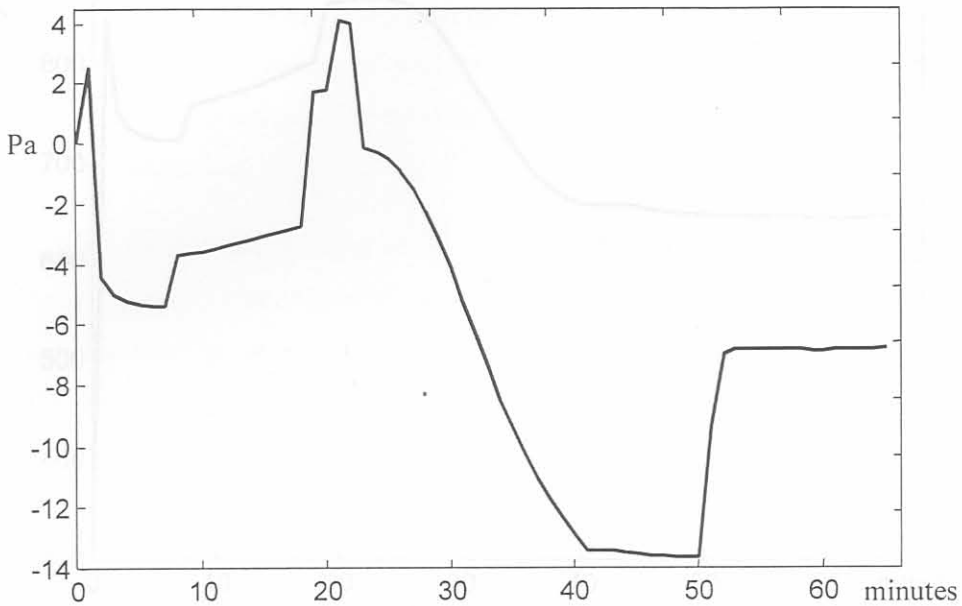

Figure 5.14 Relative Pressure

Another measured output is the steel temperature. Although it cannot be effectively controlled by means of the off-gas parameters, it is measured to adjust the model as discussed in Section 5.6. Fig.5.15 shows the off-gas carbon monoxide mass fraction at the exit of the water-cooled duct. This is also a measured output that must be limited to prevent ignition and explosion in the baghouse filter system.

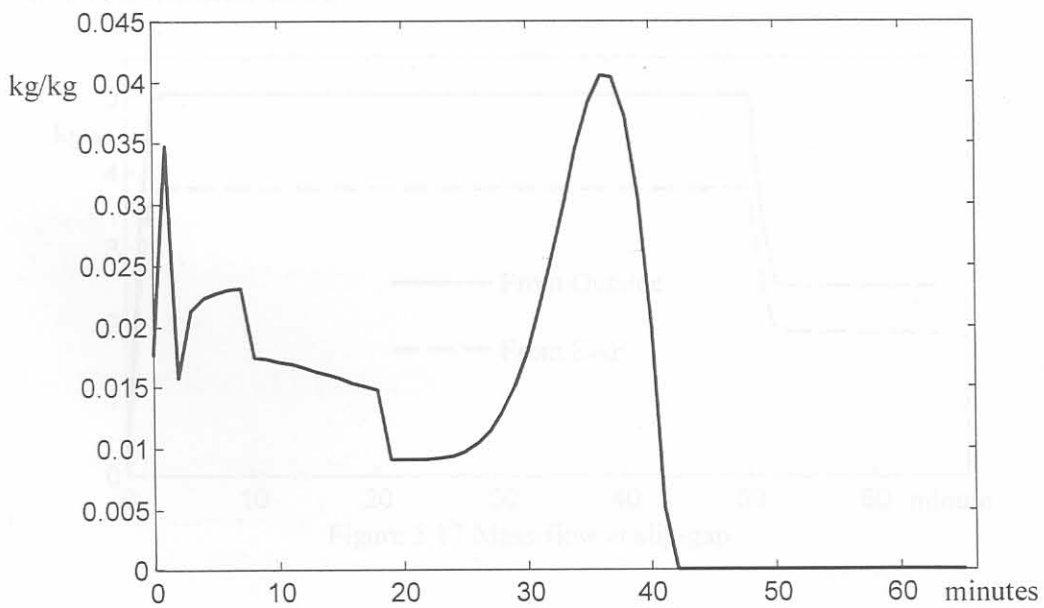

Figure 5.15 CO mass fraction in off-gas

Fig.5.16 shows the off-gas temperature, that must be limited for the same reason.

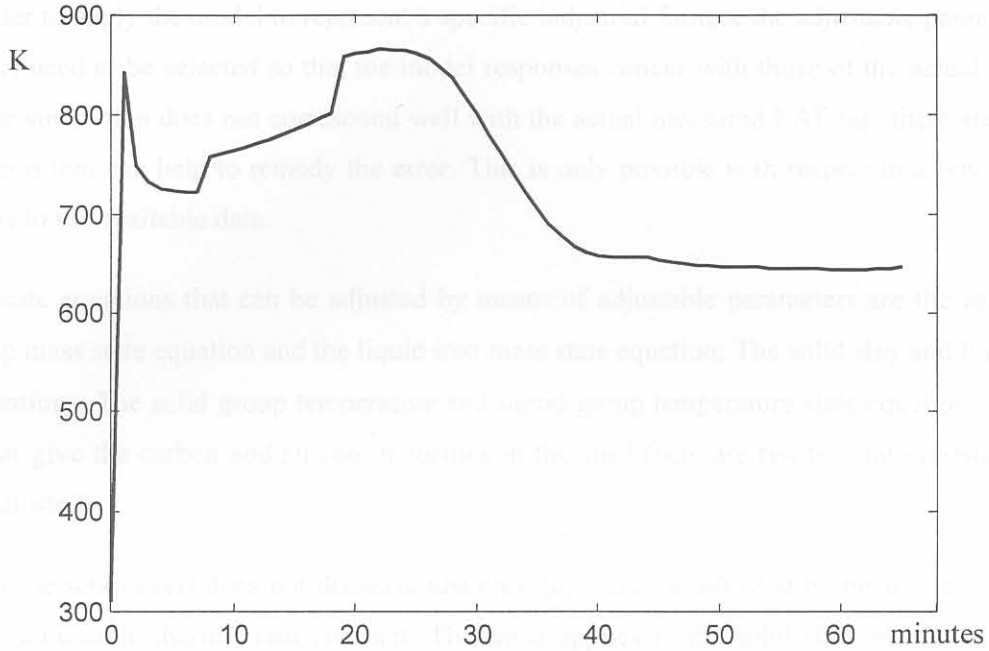

Figure 5.16 Off-gas Temperature

The mass-flow through the slip-gap and the mass-flow out of the EAF are also considered as measured outputs. Although these are not controlled variables, they can serve as model correction measurements. By means of venturi flow meters or diaphragm flow metres it is possible to measure the actual mass-flow on a plant [41]. The mass-flow measurements together with the steel temperature and furnace pressure measurements could then be used to correct the model errors. Fig.5.17 shows the two mass-flows:

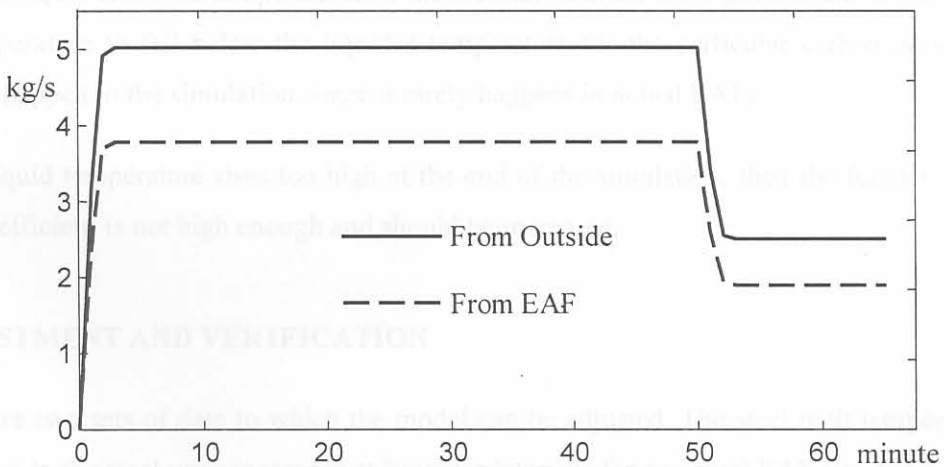

Figure 5.17 Mass-flow at slip-gap

5.5 METHOD FOR MODEL ADJUSTMENT

In order to apply the model to represent a specific industrial furnace the adjustable parameters in the model need to be selected so that the model responses concur with those of the actual furnace. When the simulation does not correspond well with the actual measured EAF tap, there are certain adjustments that can help to remedy the error. This is only possible with respect to a few selected states due to the available data.

The state equations that can be adjusted by means of adjustable parameters are the following: The scrap mass state equation and the liquid iron mass state equation; The solid slag and liquid slag state equations; The solid group temperature and liquid group temperature state equations. For the states that give the carbon and silicon impurities in the steel there are reaction rate constants that can be adjusted.

When the scrap mass does not decrease fast enough, it can be adjusted by means of increasing k_{ther1}, the adjustable thermal rate constant. The same applies to the solid slag mass (k_{ther5}). Care must however be taken not to force the solid slag mass to decrease to zero, since slag is continually charged to the furnace and the solid slag should not decrease to zero until the very last minutes of the simulation.

Increasing the thermal rate constants has the effect of raising the rates of increase of the liquid masses. Care must be taken not to increase the thermal rates too much, since it also has a direct effect on the temperatures, especially that of the liquid group. In the first minute, when the electrical power is not yet switched on, the temperature falls quickly due to the large difference between the liquid and solid temperatures. If the thermal rates are too high, it could cause the liquid group temperature to fall below the liquidus temperature for the particular carbon content. This should not happen in the simulation, since it rarely happens in actual EAFs.

If the liquid temperature rises too high at the end of the simulation, then the furnace wall heat transfer coefficient is not high enough and should be increased.

5.6 ADJUSTMENT AND VERIFICATION

There are two sets of data to which the model can be adjusted. The steel melt temperature and the %carbon in the steel were measured at irregular intervals for an actual EAF tap. Fig.5.18 shows the comparison of the %C in the steel and Fig.5.19 shows the comparison of the temperatures. These are simulations that were done before model adjustment.

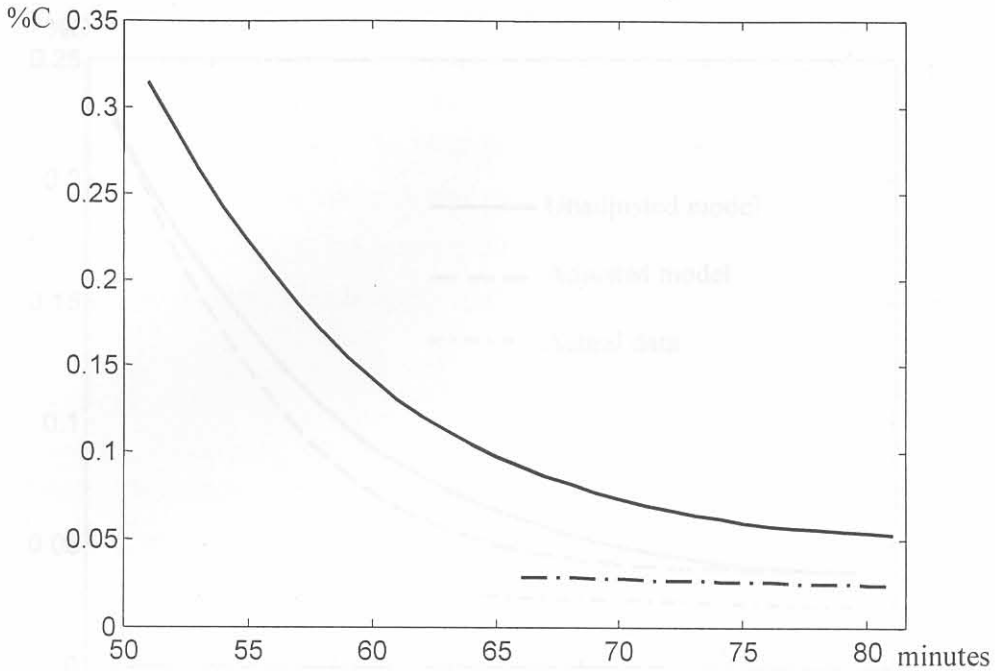

Figure 5.18 Comparison of %C given by model and actual data (dashed)

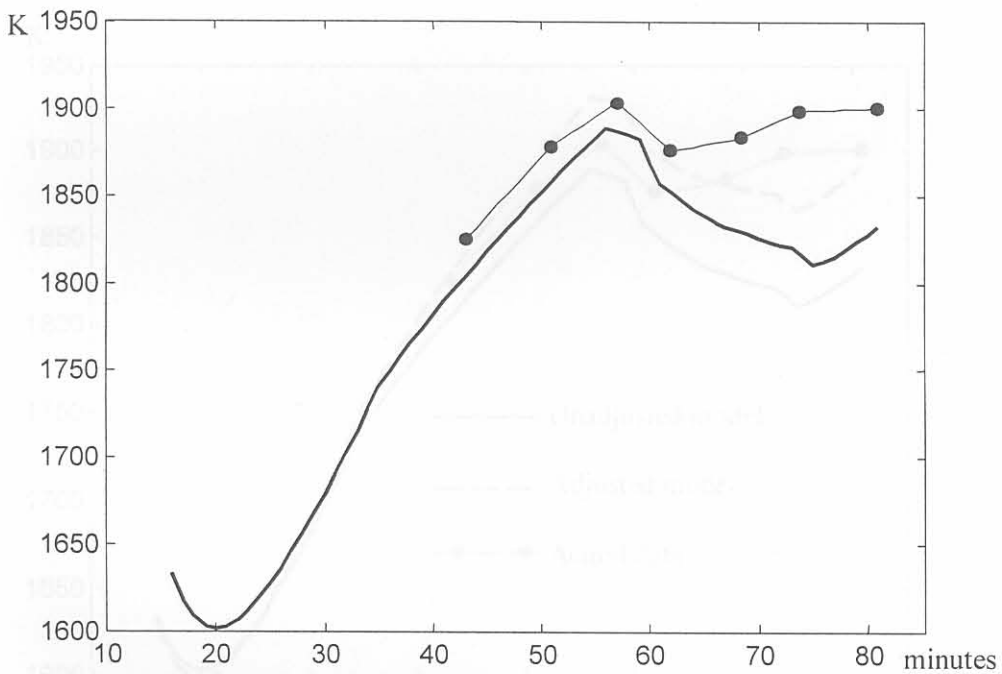

Figure 5.19 Comparison of unadjusted model temperature against actual EAF tap data temperature (dotted). Note: actual instead of simulation time

To improve the temperature correlation with the actual tap data the heat-loss coefficient for the EAF wall must be decreased. To adjust the %C the reaction rate coefficient for the C-FeO reaction must be increased. The two adjustments were done separately in that order, namely first heat-loss coefficient and then reaction rate coefficient. The heat-loss coefficient was initially 15, and was adjusted to a final value of 13.1. The reaction rate coefficient was initially 48, and was adjusted to a final value of 72. Fig.5.20 compares the adjusted model %C and Fig.5.21 the adjusted temperature.

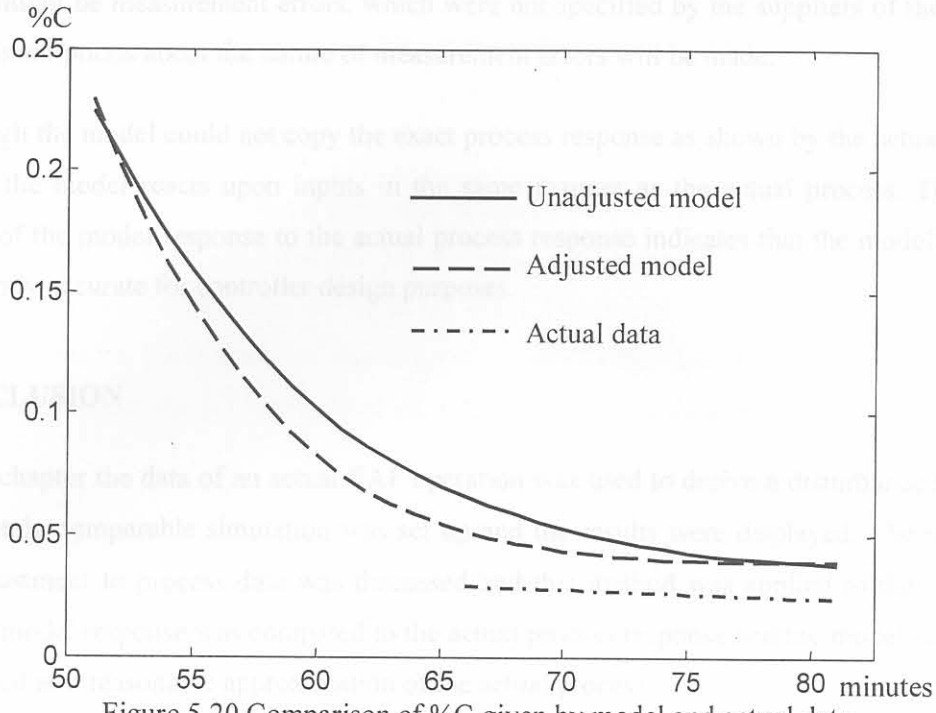

Figure 5.20 Comparison of %C given by model and actual data

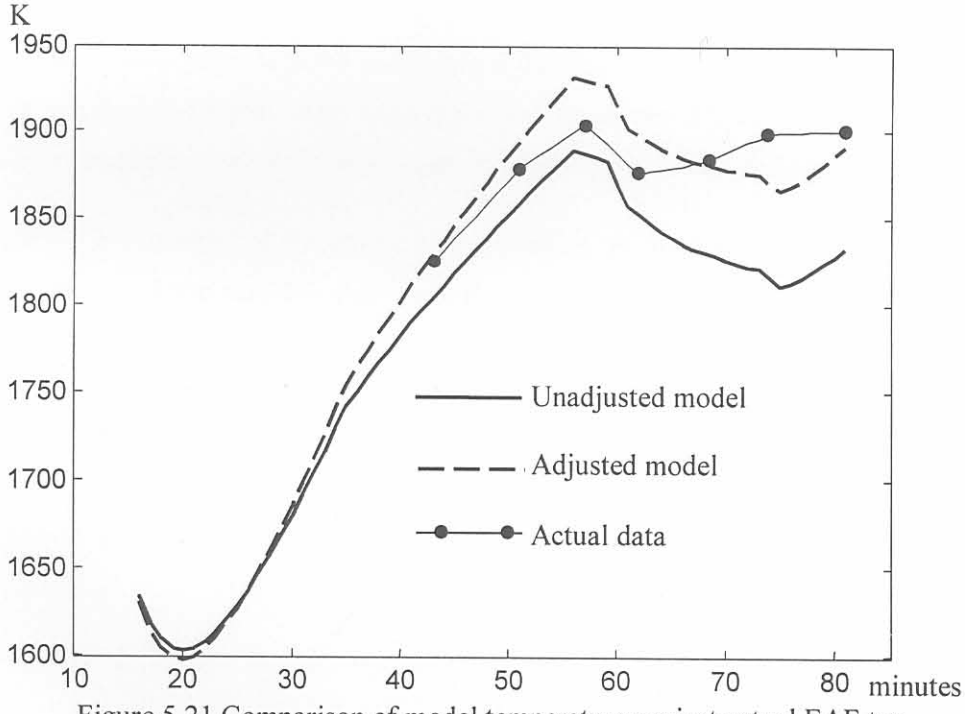

Figure 5.21 Comparison of model temperature against actual EAF tap data temperature.

The adjusted model reaches the same final temperature and achieves good correlation with the actual data. The carbon content fails to correlate as well.

While it is important that any meaningful model should represent the actual process as closely as possible, the inadequacies of the available process data must also always be taken into account.

There might be measurement errors, which were not specified by the suppliers of the data used here. No assumptions about the nature of measurement errors will be made.

Although the model could not copy the exact process response as shown by the actual data, it is clear that the model reacts upon inputs in the same manner as the actual process. The relative closeness of the model response to the actual process response indicates that the model derivation is sufficiently accurate for controller design purposes.

5.7 CONCLUSION

In this chapter the data of an actual EAF operation was used to derive a disturbance model. An approximately comparable simulation was set up and the results were displayed. The method for model adjustment to process data was discussed and this method was applied to the example at hand. The model response was compared to the actual process response and the model was verified and accepted as a reasonable approximation of the actual process.